

# **CHILD Eolian Deposition Module**

Gregory E. Tucker<sup>1</sup>, Nicole M. Gasparini, and Rafael L. Bras

Department of Civil and Environmental Engineering  
Massachusetts Institute of Technology  
Cambridge, MA 02139

Part I-G of final technical report submitted to U.S. Army Corps of Engineers  
Construction Engineering Research Laboratory (USACERL)  
by Gregory E. Tucker, Nicole M. Gasparini, Rafael L. Bras, and Stephen T. Lancaster  
in fulfillment of contract number DACA88-95-C-0017

April, 1999

---

1. To whom correspondence should be addressed: Dept. of Civil & Environmental Engineering, MIT Room 48-429, Cambridge, MA 02139, ph. (617) 252-1607, fax (617) 253-7475, email [gtucker@mit.edu](mailto:gtucker@mit.edu)

## Introduction

Deposition of wind-borne sediment is an important component of landscape dynamics in many regions, most notably regions such as the U.S. midcontinent and China's Loess Plateau, which once lay near the margins of Pleistocene ice sheets. Geomorphic studies in and around Fort Riley, Kansas, for example, have revealed that accumulations of loess make up an important component of both the Pleistocene and Holocene stratigraphic record (Johnson, 1998). From a process-geomorphic viewpoint, loess deposition provides important evidence for periods of landscape instability: a landscape having a sparse enough vegetation cover to allow for significant wind entrainment is also likely to be highly susceptible to water erosion. Moreover, the input of wind-borne sediment to a catchment is certain to have an impact on its fluvial system, though the nature of that impact remains poorly understood. Finally, wind-borne sediment will tend to bury cultural materials and thus enhance their likelihood of their preservation; the net impact of episodic loess input on the archaeological record likewise remains poorly understood.

In order to provide a theoretical tool for exploring issues such as the relationship among loess input, catchment dynamics, and the stratigraphic record, a module for loess deposition has been developed within the CHILD model. This document describes the current version of the "eolian" module and presents an example of its application.

## Eolian Deposition Model

The eolian deposition model simply assumes a steady, uniform rate of loess deposition, with a rate constant  $D_L$ . If multiple grain sizes are used, loess deposits are assumed to consist entirely of the finest size-fraction. The loess deposition module is encoded in the `tEolian` class, the code for which can be found in the files `tEolian.h` and `tEolian.cpp`.

## **Example: Application to Forsyth Creek**

An application based on Forsyth Creek, a 12 km<sup>2</sup> catchment at Fort Riley, Kansas, is used to illustrate the eolian deposition module. Ideally, one could start by reconstructing paleo-topography and then running a set of forward simulations based on an inferred geomorphic history. Unfortunately, due to the destructive nature of erosion and the difficulty in measuring erosion or sedimentation rates outside of the radiocarbon window, reconstruction of paleo-topography in this type of environment is notoriously difficult. Rather than attempting to reconstruct paleo-topography, therefore, we instead begin by simulating a catchment based on the modern topography of the Forsyth Creek catchment and an inferred long-term rate of erosion. This simulated catchment is then used as initial condition to explore the consequences of episodic loess input. Although this approach leaves out many of the details of the actual landscape, it provides a way to conduct simple controlled numerical experiments that can lead to enhanced insight into the dynamics and timing of catchment response and the associated stratigraphic record.

### **Initial Conditions**

For simplicity, we start with the assumption that our initial condition is a catchment undergoing a spatially uniform erosion rate, equal to the long-term rate of lowering at its outlet (in this case, the Kansas River). For Forsyth Creek, the uniform-erosion rate assumption is clearly a simplification. The topography along the southeast margin of Fort Riley, which is characterized by a low-relief upland surface inset by a steep-walled valley system, suggests that the fluvial systems bordering the Kansas River in this area are undergoing a transient response to accelerated erosion rates, perhaps in response to accelerated baselevel lowering on the Kansas. Nonetheless, for the sake of illustration the catchment is here treated as if it were in a condition of dynamic equilib-

rium.

Long-term incision rates on the Kansas River are not well known. Pleistocene terraces do provide some information, however. The highest and oldest of the identified terraces is the Menoken, which is thought to be early- to mid-Pleistocene (Johnson and Logan, 1990; Johnson, 1996). According to Johnson and Logan (1990), the terrace lies about 108 feet above the modern floodplain. Taking the age as mid-Pleistocene (1 Ma) yields an average lowering rate of about 33 m/my. If the Menoken is as old as earliest Pleistocene, c. 2 Ma, then this rate is halved. The next youngest terrace is the Buck Creek, which lies about 40' (12 m) above the modern floodplain (Johnson and Logan, 1990). It is considered minimally Illinoian; a fission-track-dated 600ka layer of fluviually redeposited volcanic ash in the upper fill of the Buck Creek terrace suggests that it is at least this old. Taking 600ka as a minimum age yields an average lowering rate of about 20 m/my. Thus, the terrace data suggest a long-term lowering rate on the order of a few tens of meters per million years. In this example, we adopt 20 m/my, recognizing that this is a loose approximation.

Using the detachment-limited approach (Section IB, equation 15), for a fluvial system undergoing spatially uniform erosion, the steepness of the channel system depends on the erosion rate, the effective discharge, and the detachment coefficient  $K_b$ . Analysis of DEM data for Forsyth Creek reveals a channel gradient of about  $3 \times 10^{-2}$  m/m at a drainage area of  $1 \text{ km}^2$ . Climate parameters can be approximated by averaging the modern monthly Ogden, KS, station data of Hawk (1992), which yields  $T_r = 6.8$  hours,  $T_b = 138$  hours, and  $P = 1.353$  mm/hr (this station is located west of Fort Riley and is likely therefore to underestimate total precipitation). Using the approach outlined in Section ID, and neglecting infiltration, the long-term average runoff erosion rate at a given point depends on climate, erosion, and topography according to

$$\frac{PT_r}{(T_r + T_b)} K \Gamma(m + 1) A^m S^n, \quad (1)$$

where  $A$  is drainage area,  $S$  is slope,  $\Gamma$  is the gamma function, and  $K = k_b k_t$ ,  $m = m_b p_b$ , and  $n = n_b p_b$  (see Section I-B, eq 15; the threshold term is assumed to be negligible). Exponents  $m$  and  $n$  are here assumed to be 1/2 and 1 for detachment (see Whipple and Tucker, 1999). Under spatially uniform erosion, and assuming  $Q = PA$  (which is implicit in eq 1),

$$S = \left( \frac{\dot{\epsilon}(T_r + T_b)}{K P^m T_r \Gamma(m + 1)} \right)^{\frac{1}{n}} A^{-\frac{m}{n}}, \quad (2)$$

where  $\dot{\epsilon}$  is the erosion rate (dimensions of L/T). Solving for  $K$  yields  $K = 4.62 \times 10^{-6}$ .

Long-term average sediment transport capacity (Section I-D, eq 20) is more difficult to constrain. For the sake of example, we assume that sediment transport capacity for fine sediment can be modeled using the Einstein-Brown approach, assuming a negligible grain entrainment threshold. In this case,  $\gamma \sim 1.5$ ,  $np \sim 2$  (Willgoose et al., 1991; Howard, 1994). For a uniform-erosion landscape, the sediment transport capacity coefficient  $K_f (= k_w^{(1-\alpha)} k_f k_t)$ , where  $k_w$  is a width-discharge scaling factor; see Section I-D) determines the point in the network at which the stream system will become sediment-saturated and therefore transport-limited. We have no independent data to constrain this parameter for Forsyth Creek and must therefore treat it as a free parameter. It is here set to  $4.6 \times 10^{-4}$ , which implies a transition from detachment-limited to transport-limited behavior at about  $20 \text{ km}^2$  drainage area. This parameter influences the catchment response primarily by controlling the sediment-saturation point: the smaller  $K_f$  is, the more likely deposition is to occur within the main valleys in response to sediment input.

## Loess Input

In the example shown in Figures 1–4, a steady state (constant erosion) catchment is created as an initial condition using the parameters discussed above. This initial condition is then subjected to a sequence of episodes of loess deposition, alternating with periods of no deposition. On Fort Riley, Johnson (1998) has documented alternating periods of relative landscape stability and soil formation, and loess deposition. In the late Pleistocene, a period of soil formation occurs at c. 19-24ka, represented by the Gilman Canyon formation. A period of loess deposition (Peoria loess) follows until renewed pedogenesis and landscape stability begin again at about 10.5ka (represented by the Brady soil). Loess deposition (Bignell loess) commences again around 9ka and continues intermittently throughout the Holocene. In short, the record at Fort Riley indicates episodic periods of loess deposition lasting on the order of a few thousand years. Based on this, the model is run with periods of loess deposition lasting 5000 years and separated by periods of stability (non-deposition) also lasting 5000 years. Four such cycles are simulated. Here, loess deposits are treated as “regolith,” with an erodibility coefficient an order of magnitude higher than that of the “bedrock” (representing both the limestone-shale bedrock in channels and cohesive, vegetation-armored soils on hillslopes).

The input loess deposition rate is based on data from Fort Riley. In the vicinity of Forsyth Creek, a tributary to the Kansas River, Johnson (1998) reports outcrops of Loveland and Peoria (late Quaternary) loesses, as well as scattered outcrops of Bignell (Holocene) loess. Radiocarbon dating at the Sumner Hill locality by Johnson (1998) indicates average soil accumulation rates on the order of 0.02cm/yr over time spans ranging from ~2,200 years to ~12,300 years. These figures are minima, for two reasons: (1) some fraction of the original material is likely to have been lost to erosion, and (2) the data may span intervals both of accumulation and non-accumulation.

Radiocarbon data from the Pumphouse Hill site indicate a significantly lower accumulation rate,  $\sim 0.009$  cm/yr. The record at this site is also considerable longer ( $\sim 30,000$  years) than at Sumner Hill, and the lower rate may be a function of either an early depositional hiatus(es), differing landscape position, or both. Here, a deposition rate of  $0.02$  cm/yr is used in the simulations, which implies one meter of potential accumulation during each deposition period. The results are shown in Figures 2–4.

## Results

Although the simulated deposition rate is uniform in space, because of the effects of water erosion the resulting accumulation pattern is not. Figure 2 shows the average accumulation pattern during the third simulated deposition phase. Net accumulation is greatest in the low-gradient portions of the landscape, which in this example correspond to the upland headwaters on the far left (which had not yet reached equilibrium with baselevel lowering at the time the simulation was run), and the lower portion of the basin. Reworking and redeposition of eroded material also contributes to accumulation along the lower portion of the main drainage. The steep valley side-slopes are the locations of lowest net accumulation. In these areas, a steep gradient contributes to rapid erosion of incoming sediment. By contrast, within the valley network, the erosion potential is high but is counterbalanced by the convergence of sediment from upstream and side-slopes. In this respect, the results of this simulation resemble the findings of Tucker and Slingerland (1997), who showed that accelerated denudation could lead to significant but temporary sediment accumulation within valleys resulting from convergence of upslope sediment inputs.

Figure 3 shows the patterns of erosion and deposition during the subsequent (third) period of no loess input. Here, the sediment is eroded and reworked throughout the catchment system,

with the regions of greatest erosion occurring along the upper tributaries and on steep hillslopes. This reworked sediment is then deposited within the low-gradient bottomlands near the catchment outlet. Clearly, the patterns of net deposition of both primary and reworked loess depend on the catchment topography and on the aggregation structure of the drainage system. Figure 4 illustrates the mean rate of net accumulation through time, highlighting the cyclic input. In detail, the simulations are highly dynamic, with locations and rates of erosion and deposition changing through time in response to variations in water and sediment inputs.

## **Future Improvements**

The wind deposition module provides a tool for exploring the role of eolian deposition on catchment dynamics. It uses a simple approach that could be improved with the addition of a wash load component of sediment transport, and with space-time variability in the input pattern. Most important, perhaps, would be a systematic analysis of the net impact of episodic eolian input on the general characteristics of fluvial response, and the degree to which that response depends on factors such as climate, hillslope hydrology, and catchment topography. The implications for the alluvial stratigraphic record and its associated cultural resources could be further developed, as could a more thorough comparison with the stratigraphic record at Fort Riley and elsewhere.

## **References**

- Hawk, K.L., 1992, Climatology of station storm rainfall in the continental United States: parameters of the Bartlett-Lewis and Poisson rectangular pulses models, unpublished M.S. thesis, Department of Civil and Environmental Engineering, Massachusetts Institute of Technology, 330pp.
- Howard, A.D., 1994, A detachment-limited model of drainage basin evolution: *Water Resources Research*, v. 30, p. 2261-2285.
- Johnson, D.L., 1996, A Geomorphological, Pedological, and Geoarchaeological Study of Fort Riley, Kansas, Final Geotechnical Report submitted to U.S. Army Construction Engineering Research Laboratory.



- Johnson, W.C., 1998, Paleoenvironmental Reconstruction at Fort Riley, Kansas, 1998 Phase, Technical Report submitted to U.S. Army Construction Engineering Research Laboratory.
- Johnson, W.C., and Logan, 1990, Geoarchaeology of the Kansas River Basin, central Great Plains, in Lasca, N.P., and Donohue, J., eds., Archaeological Geology of North America: Geological Society of America, Decade of North American Geology Centennial Special Volume 4, p. 267-299.
- Tucker, G.E., and Slingerland, R.L., 1997, Drainage basin response to climate change: Water Resources Research, v. 33, no. 8, p. 2031-2047.

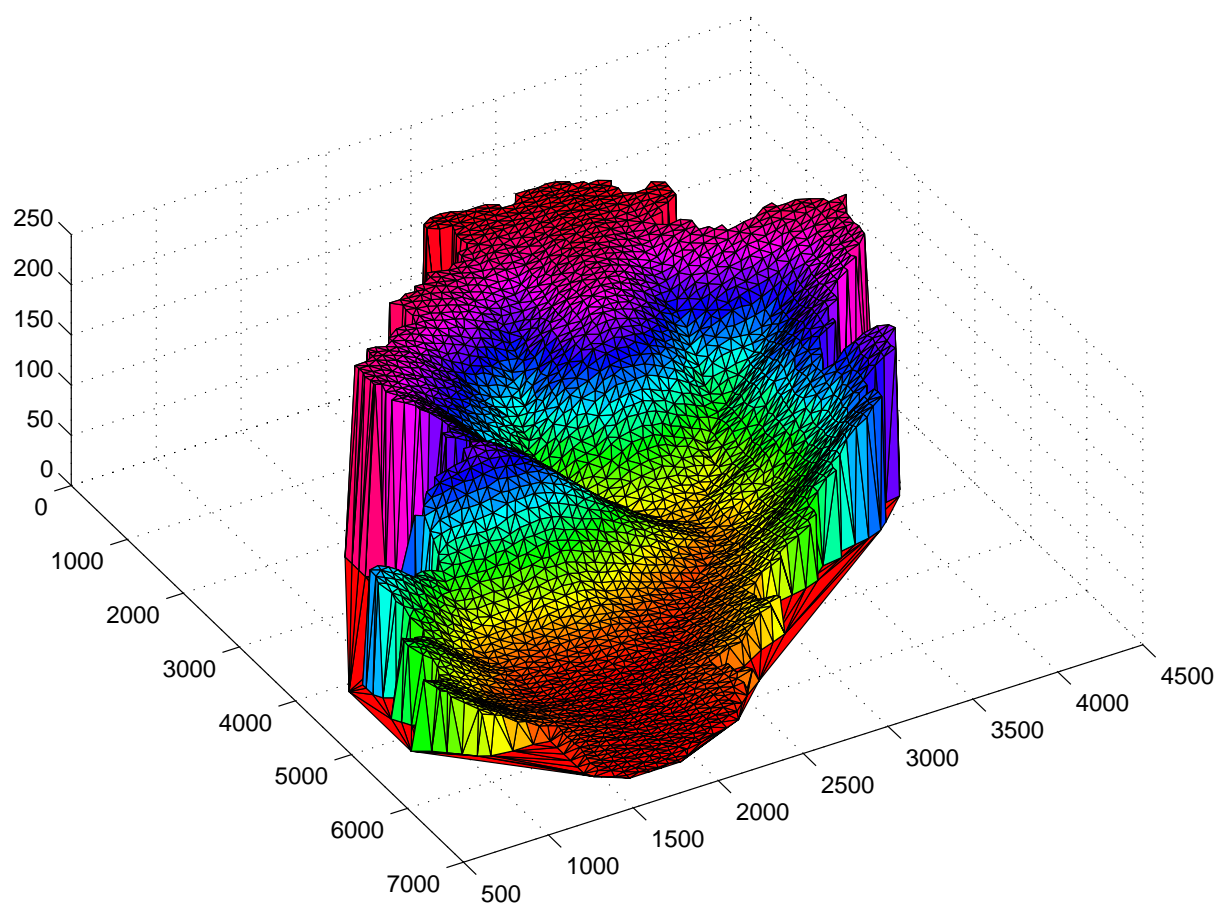


**FIGURE 1. Initial topography used in eolian input simulation (dimensions in meters).**

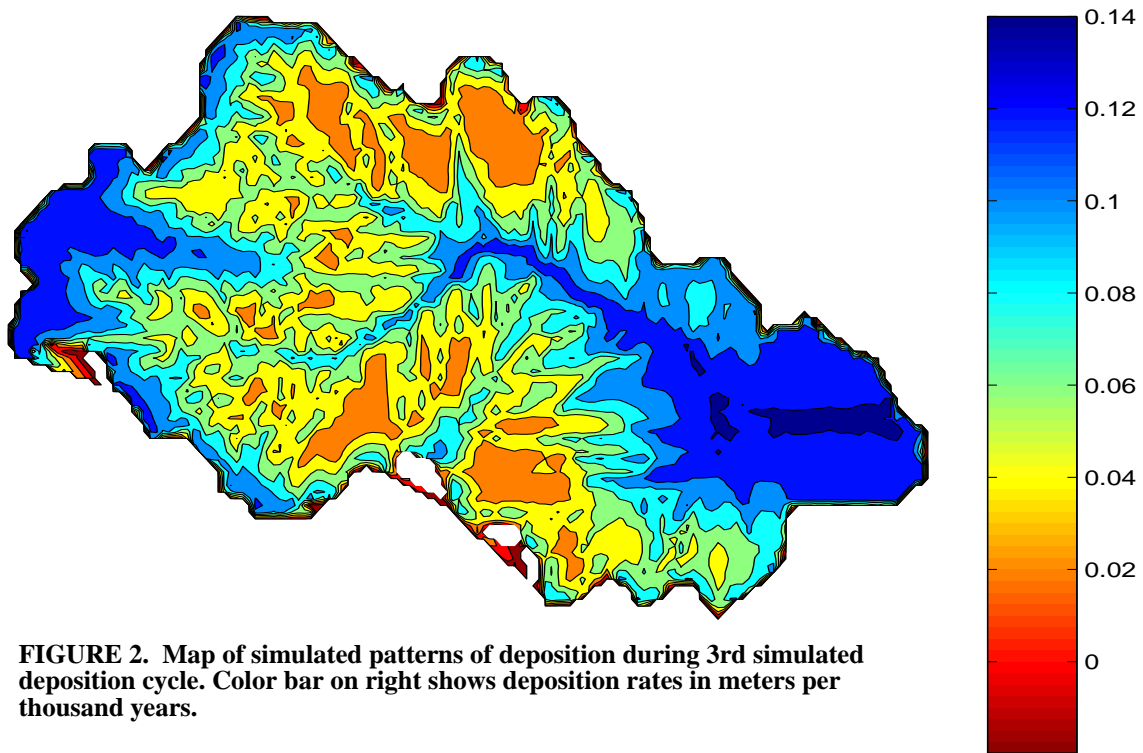


**FIGURE 2.** Map of simulated patterns of deposition during 3rd simulated deposition cycle. Color bar on right shows deposition rates in meters per thousand years.

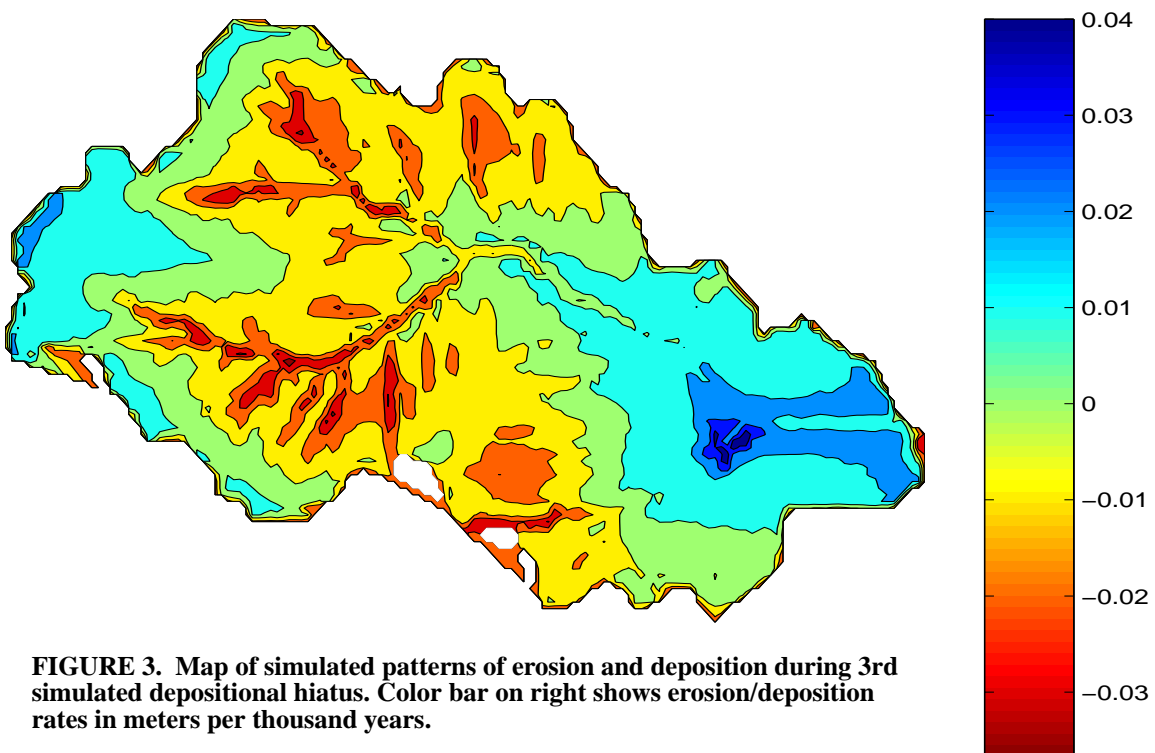


**FIGURE 3.** Map of simulated patterns of erosion and deposition during 3rd simulated depositional hiatus. Color bar on right shows erosion/deposition rates in meters per thousand years.

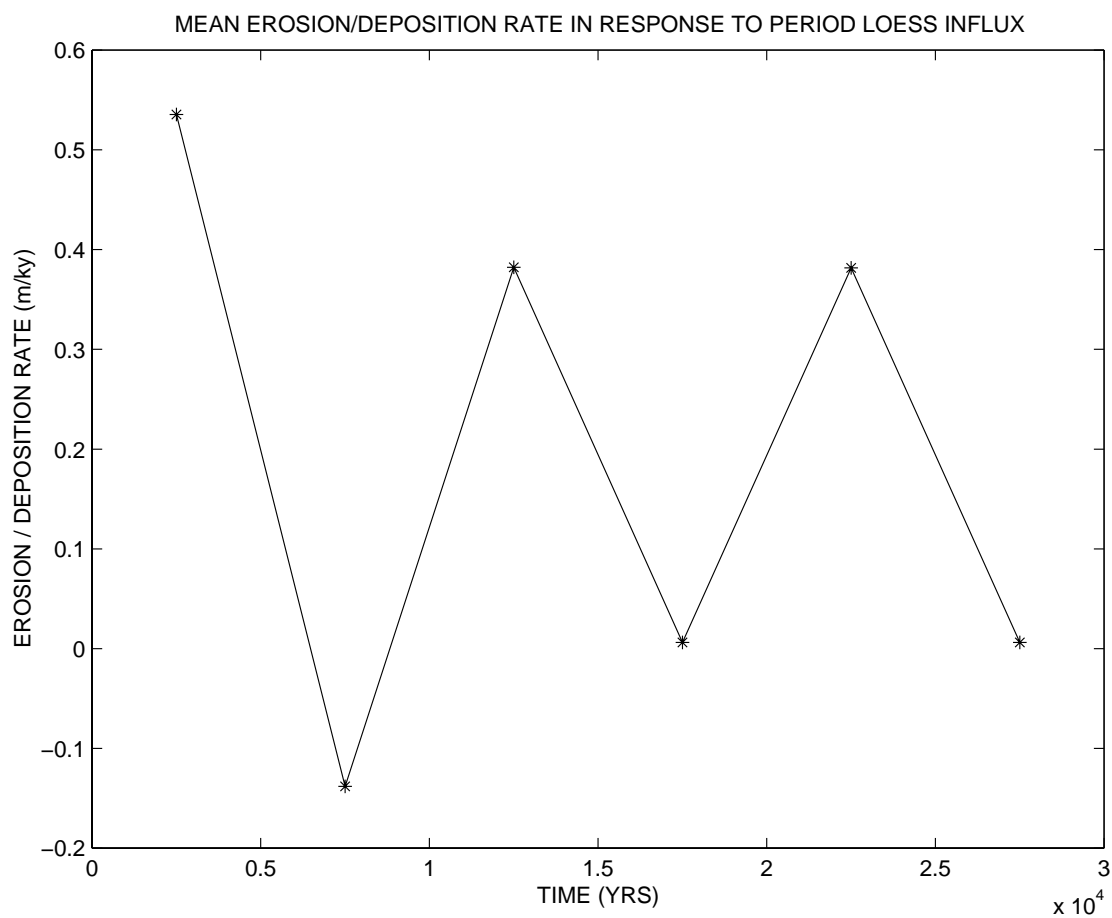


**FIGURE 4.** Mean catchment-wide net deposition (or erosion, if negative) rate versus time in eolian deposition simulation. Each symbol represents a 5,000-year average.